Transactions of NAMP 22, (2025) 97-114

Transactions of
The Nigerian Association of
Mathematical Physics
Journal homepage: https://nampjournals.org.ng

MATHEMATICAL MODELING OF HUMAN AFRICAN TRYPANOSOMIASIS (HAT) TRANSMISSION DYNAMICS WITH TWO STAGES OF INFECTION

[1]Adama, P. W., *[2]Dotia, A. K., [3]Ibrahim, M. O., [1]Aliu, T. O. and [1]Ngwu, R.

[1]Department of Mathematics and Statistics, Kwara State University, Malete, Kwara State, Nigeria

[2]Department of Mathematics, Nigerian Army University Biu, Biu, Borno State, Nigeria

[3]Department of Mathematics, University of Ilorin, Ilorin, Kwara State, Nigeria

ARTICLE INFO

Article history:
Received 18/6/2025
Revised 28/5/2025
Accepted 7/7/2025
Available online 17/7/2025

Keywords:
Mathematical model,
Stability analysis,
Basic reproduction number,
Relapse,
Sensitivity analysis

ABSTRACT

Human African Trypanosomiasis (HAT), or sleeping sickness, transmitted by tsetse flies, remains a major health threat in sub-Saharan Africa. This study developed and analysed a mathematical model to better understand HAT transmission dynamics between humans and flies. The model accounts for potential relapse in infected individuals. Ensuring realistic predictions through the positivity and boundedness checks. Stability analysis is determined. Central to our analysis is the basic reproduction number, R_0, which tells us whether HAT will spread or decline. Sensitivity analysis identified key parameters influencing the transmission pattern. Visual graphs illustrated these findings effectively. Results suggest that increasing the death rate of tsetse flies can substantially curb the spread of HAT. The study emphasises that controlling the disease requires a multifaceted approach: public health education, vector control, improved healthcare access, and investment in vaccines. These strategies are vital for the goal of eliminating HAT and enhancing health outcomes in affected regions.

1. INTRODUCTION

Human African trypanosomiasis, often called sleeping sickness, is a serious health issue in parts of sub-Saharan Africa. It's caused by tiny parasites known as Trypanosoma brucei, which people can catch when bitten by tsetse flies. In their study, [1] introduced a deterministic model that examines how HAT spreads. They explored the interactions between humans, cattle, and tsetse flies involved in transmission and provided insights into the basic reproduction number, R_0. Their findings indicate that when $R_0 < 1$, a stable disease-free state is achievable, suggesting potential strategies for controlling this challenging disease.

*Corresponding author: DOTIA, A. K.
E-mail address: akdotia@gmail.com
https://doi.org/10.60787/tnamp.v22.556

HAT progresses through two main stages: the hemolymphatic phase and the meningoencephalitic phase. Research by [2] highlights the unique clinical features and pathophysiological processes of these stages. The first stage, known as the hemolymphatic phase, often presents mild, nonspecific symptoms, such as fever, headaches, and swollen lymph nodes. This phase can persist for several months or even years, during which the disease may go undiagnosed due to its relatively mild nature. Despite the subtle symptoms, individuals in this stage can still transmit the parasite to tsetse flies, helping to sustain the cycle of infection. As the disease advances, the parasite invades the central nervous system, leading to the second stage, known as the meningoencephalitis phase. This critical stage is characterised by severe neurological symptoms, including psychiatric disorders and sleep disturbances, which is why the disease is referred to as" sleeping sickness." If left untreated, it can lead to fatal complications. Notably, some individuals can harbour the infection asymptomatically for 5 to 15 years, serving as long-term reservoirs that pose a significant risk for ongoing disease transmission within affected communities.

Understanding these stages is essential for effective disease management, as early detection and treatment can prevent long-term neurological damage and reduce transmission rates. In the hemolymphatic stage, parasites circulate through the bloodstream and lymphatic system, causing nonspecific symptoms. When the disease progresses to the meningoencephalitis stage, the neurological symptoms can be life-threatening if not addressed in time. Investigations by [3] emphasise the differences between the two stages, noting that the first stage involves systemic infection with generalised symptoms. The second stage marks a severe progression with a significantly increased mortality risk.

Using mathematical models has become a helpful way to understand how diseases like sleeping sickness spread. For example, the Susceptible-Infected-Recovered (SIR) model helps researchers see how the disease moves through populations, evaluate how different control measures might work, and guide decisions to improve public health efforts. The pioneering work of [4] laid the groundwork for this approach, facilitating a deeper exploration of the interactions among the host, the parasite, and the vector.

Numerous studies have since built on this foundation. [5] emphasized the importance of the basic reproduction number R_0 for estimating a disease's spread potential. [6] modelled disease transmission through social connections, while [7] evaluated vaccination impacts on controlling disease spread. Further studies, including those by [8], assessed the effectiveness of containment measures through quarantine and isolation. [9], [10] and [11], all addressing the broader public health challenges posed by vector-borne diseases.

Recent studies, such as those by [12], have developed optimal control models for HAT, aiming to minimize both control costs and the prevalence of infection among humans, cattle, and tsetse flies. Their findings suggest that an integrated strategy, combining healthcare education, effective treatment, and targeted vector control, offers the best promise for managing the disease. Moreover, [13] and [14], [15] explored seven-compartmental models: the SEIR model for humans and the SEI model for vectors, evaluating the effectiveness of various intervention strategies.
This article seeks to develop and analyze a comprehensive model that reflects the complexities of Human African Trypanosomiasis (HAT). It builds upon the work in [14] by incorporating two stages of infection within the human population and relapse, thereby enhancing the model's robustness and overall coverage. The model divides the human population into five groups (SEI_1I_2R) to reflect the two different infectious stages, along with a separate SEI model for the vector (the tsetse flies). By incorporating real-world data, we hope to identify the main factors that influence how the disease spreads and to evaluate how effective different intervention strategies

might be. Ultimately, our goal is to deepen the understanding of HAT's behavior and provide a strong scientific foundation to support future efforts in disease control and public health.

Here's how the paper is organized: Section 2 explains how we built the model, ensuring that its predictions make biological sense, that solutions stay positive and within reasonable bounds. It also discusses the points where the disease could potentially disappear or become steady in the population, as well as the key number (R_0) that tells us whether the disease will spread or fade away. We also analyze the stability of these states. Section 3 looks at how sensitive the model is to different parameters, meaning we see which factors have the biggest impact on disease spread. Section 4 covers the results from running computer simulations using real data, along with discussions about what these findings mean. Lastly, Section 5 wraps up with our main conclusion.

2. Materials and Methods

2.1 Model Formation

A mathematical model that describes the effect of vector-borne diseases on hosts and vectors was developed. To better understand how the disease spreads, we divided the human population into five groups: Susceptible humans (S_h) those who can catch the disease, Exposed humans (E_h) those who have been infected but aren't infectious yet, Stage one infected humans (I_{h1}) early-stage infectious individuals, Stage two infected humans (I_{h2}) individuals in the later stage of infection and recovered humans (R_h) those who have recovered and gained some immunity. Similarly, the tsetse fly vector population is divided into three groups: Susceptible flies (S_v) those that can become infected, Exposed flies (E_v) — flies that have been infected but are not yet able to transmit the disease and Infected flies (I_v) the flies capable of spreading the disease.

We denote the total human population at time t as ($N_h(t)$) and the total fly population as ($N_v(t)$)). Table 1 provides details on other parameters used in the model, which are also summarized in the schematic diagram shown in Figure 1.

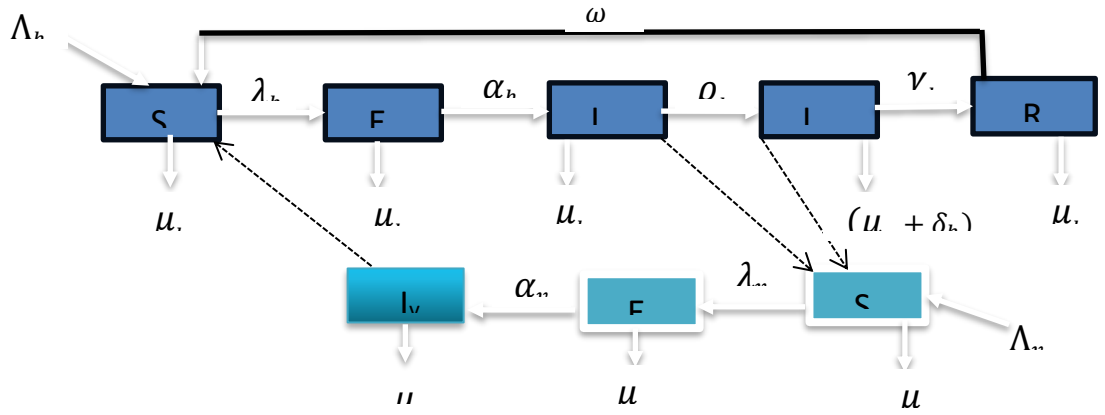

$$
\begin{aligned}
\frac{dS_h}{dt} &= \Lambda_h + \omega R_h - \beta_h S_h I_v - \mu_h S_h \\
\frac{dE_h}{dt} &= \beta_h S_h I_v - (\alpha_h + \mu_h) E_h \\
\frac{dI_{h1}}{dt} &= \alpha_h E_h - (\rho_h + \mu_h) I_{h1} \\
\frac{dI_{h2}}{dt} &= \rho_h I_{h1} - (\gamma_h + \delta_h + \mu_h) I_{h2} \\
\frac{dR_h}{dt} &= \gamma_h I_{h2} - (\omega + \mu_h) R_h \\
\frac{dS_v}{dt} &= \Lambda_v - \beta_v S_v (I_{h1} + I_{h2}) - \mu_v S_v \\
\frac{dE_v}{dt} &= \beta_v S_v (I_{h1} + I_{h2}) - (\alpha_v + \mu_v) E_v \\
\frac{dI_v}{dt} &= \alpha_v E_v - \mu_v I_v
\end{aligned}
\qquad (1)
$$

Table 1: Notation and description of variables and parameters

Notation	Description of variables and parameters
$S_h(t)$	The total number of people who are vulnerable to infection at time t
$E_h(t)$	The total number of people who are exposed to infection at time t
$I_{h1}(t)$	The number of people in the early stage of infection at time *t*
$I_{h2}(t)$	The number of people in the late stage of infection at time *t*
$R_h(t)$	The total number of people who have recovered from infection at time t
$S_v(t)$	The total number of tsetse flies susceptible at time t
$E(t)$	The total number of tsetse flies exposed at time t
$I_v(t)$	The total number of tsetse flies infected at time t
Λ_h	The rate at which new people join the human population
Λ_v	The rate at which new people join the tsetse fly population
δ_h	Disease-induced death
μ_h	The regular rate at which humans die naturally
μ_V	The regular rate at which tsetse flies die naturally.
β_h	The rate at which humans become exposed to the disease.
β_v	The rate at which the vulnerable tsetse fly becomes exposed to the disease
α_h	The rate at which human Progresses from exposure to the early stage of infection
α_v	The rate at which the exposed tsetse fly gets infected
ρ_h	The rate at which human Progresses from the early stage of infection to the late stage
γ_h	The recovery rate of humans
ω	The rate at which the recovered lose their immunity and become vulnerable again.

$$N_h = S_h + E_h + I_{h1} + I_{h2} + R_h \tag{2}$$

$$N_v = S_v + E_v + I_v \tag{3}$$

Invariant Region of the Model

By adding the system of equations (1), we have:

$$\frac{dN_h}{dt} = \frac{dS_h}{dt} + \frac{dE_h}{dt} + \frac{dI_{h2}}{dt} + \frac{dI_{h1}}{dt} + \frac{dR_h}{dt} = \Lambda_h - (\delta_h + \mu_h)N_h \tag{4}$$

and

$$\frac{dN_h}{dt} = \frac{dS_h}{dt} + \frac{dE_h}{dt} + \frac{dI_{h2}}{dt} + \frac{dI_{h1}}{dt} + \frac{dR_h}{dt} = \Lambda_h - \mu_h N_v \tag{5}$$

Theorem 1

The basic dynamic features of these model equations (1) have solutions which are contained in the feasible region

$\Omega = \Omega_h \times \Omega_v$ for all $t > 0$

Proof

Let

$$\Omega = (S_h, E_h, I_{h1}, I_{h2}, R_h, S_v, E_v, I_v) \epsilon \Re_+^8 \tag{6}$$

with non-negative initial conditions using the differential inequality theorem, Birkhoff and Rota (1978) on equation (4). When there are no deaths caused by the disease in the human population, equation (4) becomes,

$$\frac{d\boldsymbol{N_v}}{dt} \leq \Lambda_h - \mu_h N_h \tag{7}$$

It follows that

$$0 \leq N_h \leq \frac{\boldsymbol{\Lambda_h}}{\mu_h}, \tag{8}$$

hence

$$\Lambda_h - \mu_h N_h \geq K e^{-\mu_h t} \tag{9}$$

Where K is the constant

Similarly, for the vector population equation, (5) becomes,

$$\Lambda_v - \mu_v N_v \geq K e^{-\mu_v t} \tag{10}$$

Where K is the constant

Therefore, all feasible solutions of the human and vector of the system model are in the regions:

$$\Omega = \{(S_h, E_h, I_{h1}, I_{h2}, R_h) \epsilon \Re_+^5 : S_h, E_h, I_{h1}, I_{h2}, R_h \geq 0, N_h \leq \Lambda_h - \mu_h N_h\} \tag{11}$$

$$\Omega = \{(S_v, E_v, I_v) \epsilon \Re_+^3 : S_v, E_v, I_v \geq 0, N_v \leq \Lambda_v - \mu_v N_v\} \tag{12}$$

Thus, the feasible set of the model is given by

$$\Omega = \{(S_h, E_h, I_{h1}, I_{h2}, R_h, S_v, E_v, I_v) \epsilon \Re_+^8 : S_h, E_h, I_{h1}, I_{h2}, R_h, S_v, E_v, I_v \geq 0; N_h \leq \frac{\boldsymbol{\Lambda_h}}{\mu_h}, N_v \leq \frac{\boldsymbol{\Lambda_v}}{\mu_v}\} \tag{13}$$

This means the model is positively invariant, so the solutions stay positive at all times, and it makes sense biologically and is mathematically well-structured.

2.2 Positivity and Boundedness of the Solutions

In this subsection, we show the positivity and boundedness of the system equation (1) above.

Lemma 1

Let the initial data be

$$\left\{\left(S_h(0), E_h(0), I_{h1}(0), I_{h2}(0), R_h(0), S_v(0), E_v(0), I_v(0)\right) \geq 0\right\} \epsilon \Omega \tag{14}$$

Then, the solution set

$\{S_h(t) + E_h(t) + I_{h1}(t) + I_{h2}(t) + R_h(t) + S_v(t) + E_v(0) + I_v(t)\}$ of the system (1) is positive for all $t > 0$.

proof

From the system of equations (1) above, we solve the following

$$\frac{dS_h}{dt} = \Lambda_h + \omega R_h - \beta_h S_h I_v - \mu_h S_h \geq \Lambda_h - \mu_h S_h \quad (15)$$

$$\frac{dS_h}{dt} \geq \Lambda_h - \mu_h S_h \quad (16)$$

$$\frac{dS_h}{dt} + \mu_h S_h \geq \Lambda_h \quad (17)$$

using integrating factors, we have

$$\frac{d}{dt}(S_h e^{\mu_h t}) \geq \Lambda_h e^{\mu_h t} \quad (18)$$

$$S_h(t) e^{e^{\mu_h t}} \geq \frac{\Lambda_h}{\mu_h} e^{\mu_h t} + C \quad (19)$$

$$S_h(t) \geq \frac{\Lambda_h}{\mu_h} + C e^{-\mu_h t} \quad (20)$$

Hence substituting $t = 0$, we have $S_h(0) \geq \frac{\Lambda_h}{\mu_h} + C \Rightarrow C \leq S_h(0) - \frac{\Lambda_h}{\mu_h}$ (21)

Which gives,

$$S_h(t) \geq \frac{\Lambda_h}{\mu_h} + (S_h(0) - \frac{\Lambda_h}{\mu_h}) e^{\mu_h t} > 0 \quad (22)$$

From equation (1) also,

$$\frac{dE_h}{dt} = \beta_h S_h I_v - (\alpha_h + \mu_h) E_h \geq -(\alpha_h + \mu_h) E_h \quad (23)$$

$$\int \frac{dE_h}{dt} \geq -\int (\alpha_h + \mu_h) dt \quad (24)$$

Integrating gives:

$$E_h(t) \geq E_h(0) e^{-(\alpha_h + \mu_h)t} > 0 \quad (25)$$

Similarly, from equation (1) we have

$$I_{h1}(t) \geq I_{h1}(0) e^{-(\rho_h + \mu_h)t} > 0 \quad (26)$$

$$I_{h2}(t) \geq I_{h2}(0) e^{-(\gamma_h + \delta_h + \mu_h)t} > 0 \quad (27)$$

$$R_h(t) \geq R_h(0) e^{-(\omega + \mu_h)t} > 0 \quad (28)$$

$$S_v(t) \geq \frac{\Lambda_v}{\mu_v} + (S_v(0) - \frac{\Lambda_v}{\mu_v})e^{\mu_v t} > 0 \quad (29)$$

$$E_v(t) \geq E_v(0)e^{-(\alpha_v+\mu_v)t} > 0 \quad (30)$$

$$I_v(t) \geq I_v(0)e^{-\mu_v t} > 0 \quad (31)$$

Therefore, all the solutions of the system of equations (1) are positive for all $t > 0$.

2.3 Equilibrium Points of the Model

At equilibrium, we have

$$\frac{dS_h}{dt} = \frac{dE_h}{dt} = \frac{dI_{h1}}{dt} = \frac{dI_{h2}}{dt} = \frac{dR_h}{dt} = \frac{dS_v}{dt} = \frac{dE_v}{dt} = \frac{dI_v}{dt} = 0 \quad (32)$$

2.3.1 HAT-Free Equilibrium State

Let

$$(S_h, E_h, I_{h1}, I_{h2}, R_h, S_v, E_v, I_v) = (S_h^0, E_h^0, I_{h2}^0, I_{h1}^0, R_h^0, S_v^0, E_v^0, I_v^0) \quad (33)$$

To find the HAT-free equilibrium (HAT-FE) of the given system of differential equations, we set the whole compartment to zero, and since the HAT-free equilibrium, there are no infected individuals. we set $E_h = I_{h1} = I_{h2} = E_v = I_v = 0$ and then solve for the remaining compartments.

Therefore, the system (1) becomes

$$(S_h^0, E_h^0, I_{h2}^0, I_{h1}^0, R_h^0, S_v^0, E_v^0, I_v^0) = \left(\frac{\Lambda_h}{\mu_h}, 0,0,0,0, \frac{\Lambda_v}{\mu_v}, 0,0\right) \quad (34)$$

2.3.2 HAT-Endemic Equilibrium State

Let

$$(S_h, E_h, I_{h1}, I_{h2}, R_h, S_v, E_v, I_v) = (S_h^*, E_h^*, I_{h2}^*, I_{h1}^*, R_h^*, S_v^*, E_v^*, I_v^*) \quad (35)$$

and

$$A_1 = (\alpha_h + \mu_h), A_2 = (\rho_h + \mu_h), A_3 = (\gamma_h + \delta_h + \mu_h), A_4 = (\omega + \mu_h), A_1 = (\alpha_v + \mu_v)$$

Then,

$$\left.\begin{aligned}
S_h^* &= A_1A_2A_3A_5\mu_v\left(\frac{A_1A_2A_3A_4\mu_v+A_3A_4\beta_v\Lambda_h\alpha_h+A_4\rho_h\beta_v\Lambda_h\alpha_h-\mu_v\omega\rho_h\gamma_h\alpha_h}{(A_1A_2A_3A_4A_5\mu_v\mu_h+A_1A_2A_3A_4\beta_h\Lambda_v\alpha_v-\beta_h\omega\rho_h\Lambda_v\alpha_h\alpha_v\gamma_h)\beta_v\alpha_h(A_3+\rho_h)}\right),\\
E_h^* &= A_2A_3A_5\mu_v\left(\frac{A_1A_2A_3A_4\mu_h\mu_v^2+A_3\beta_h\beta_v\Lambda_h\Lambda_v\alpha_h\alpha_v+\rho_h\beta_h\beta_v\Lambda_h\Lambda_v\alpha_h\alpha_v}{(A_1A_2A_3A_4A_5\mu_v\mu_h+A_1A_2A_3A_4\beta_h\Lambda_v\alpha_v-\beta_h\omega\rho_h\Lambda_v\alpha_h\alpha_v\gamma_h)\beta_v\alpha_h(A_1+\rho_h)}\right),\\
I_{h1}^* &= A_3A_4\left(\frac{A_1A_2A_3A_4\mu_h\mu_v^2+A_3\beta_h\beta_v\Lambda_h\Lambda_v\alpha_h\alpha_v+\rho_h\beta_h\beta_v\Lambda_h\Lambda_v\alpha_h\alpha_v}{(A_1A_2A_3A_4A_5\mu_v\mu_h+A_1A_2A_3A_4\beta_h\Lambda_v\alpha_v-\beta_h\omega\rho_h\Lambda_v\alpha_h\alpha_v\gamma_h)\beta_v(A_3+\rho_h)}\right),\\
I_{h2}^* &= A_2\rho_h\left(\frac{A_1A_2A_3A_4\mu_h\mu_v^2+A_3\beta_h\beta_v\Lambda_h\Lambda_v\alpha_h\alpha_v+\rho_h\beta_h\beta_v\Lambda_h\Lambda_v\alpha_h\alpha_v}{(A_1A_2A_3A_4A_5\mu_v\mu_h+A_1A_2A_3A_4\beta_h\Lambda_v\alpha_v-\beta_h\omega\rho_h\Lambda_v\alpha_h\alpha_v\gamma_h)\beta_v\alpha_h(A_1+\rho_h)}\right),\\
R_h^* &= A_2\rho_h\left(\frac{A_1A_2A_3A_4\mu_h\mu_v^2+A_3\beta_h\beta_v\Lambda_h\Lambda_v\alpha_h\alpha_v+\rho_h\beta_h\beta_v\Lambda_h\Lambda_v\alpha_h\alpha_v}{(A_1A_2A_3A_4A_5\mu_v\mu_h+A_1A_2A_3A_4\beta_h\Lambda_v\alpha_v-\beta_h\omega\rho_h\Lambda_v\alpha_h\alpha_v\gamma_h)\beta_v\alpha_h(A_1+\rho_h)}\right),\\
S_v^* &= \left(\frac{A_1A_2A_3A_4A_5\mu_h\mu_v+A_1A_2A_3A_4\beta_h\Lambda_v\alpha_v-\omega\rho_h\gamma_h\alpha_h\beta_h\Lambda_v\alpha_v}{\beta_h\alpha_v(A_1A_2A_3A_4\mu_v+A_3A_4\beta_v\Lambda_h\alpha_h+A_4\rho_h\beta_v\Lambda_h\alpha_h-\mu_v\omega\rho_h\Lambda_v\alpha_h\gamma_h)}\right),\\
E_v^* &= A_4\left(\frac{A_1A_2A_3A_5\mu_h\mu_v^2+A_3\beta_v\alpha_h\Lambda_h\beta_h\Lambda_v\alpha_v+\rho_h\beta_h\beta_v\Lambda_h\Lambda_v\alpha_h\alpha_v}{\beta_h\alpha_v(A_1A_2A_3A_4\mu_v+A_3A_4\beta_v\Lambda_h\alpha_h+A_4\rho_h\beta_v\Lambda_h\alpha_h-\mu_v\omega\rho_h\Lambda_v\alpha_h\gamma_h)A_5}\right),\\
I_v^* &= A_4\left(\frac{A_1A_2A_3A_4A_5\mu_h\mu_v^2+A_1A_2A_3A_4\beta_h\Lambda_v\alpha_v+\rho_h\beta_h\beta_v\Lambda_h\Lambda_v\alpha_h\alpha_v}{\beta_h\mu_v(A_1A_2A_3A_4\mu_v+A_3A_4\beta_v\Lambda_h\alpha_h+A_4\rho_h\beta_v\Lambda_h\alpha_h-\mu_v\omega\rho_h\Lambda_v\alpha_h\gamma_h)A_5}\right)
\end{aligned}\right\} \quad (36)$$

2.4 The Basic Reproduction Number

The basic reproduction number, known as R_0, is a key idea in studying how infectious diseases spread. It helps us understand whether a disease is likely to take hold and spread through a population or die out on its own.

To calculate R_0, scientists often use a method called the next-generation matrix approach, which was first introduced by [5] and subsequently refined by[16]. R_0 is very important for predicting the stability of a disease-free state, meaning when no one is infected. If R_0 is less than 1, the disease-free state is stable, and the infection is unlikely to spread. But if R_0 is greater than 1, the disease can invade and potentially become endemic in the population.

Mathematically, R_0 is defined as the spectral radius (i.e., the dominant eigenvalue) of the matrix product FV^{-1}, expressed as:

$$R_0 = \rho(FV^{-1}) \quad (37)$$

where ρ denotes the spectral radius.

$$f_i(x) = \begin{pmatrix} \beta_h S_h I_v \\ 0 \\ \beta_v S_v (I_{h1} + I_{h2}) \\ 0 \\ 0 \end{pmatrix} \quad (38)$$

$$v_i(x) = \begin{pmatrix} A_1 E_h \\ -\alpha_h E_h + A_2 I_{h1} \\ -\rho_h I_{h1} + A_3 I_{h2} \\ A_5 E_v \\ -\alpha_v E_v + \mu_v I_v \end{pmatrix} \quad (39)$$

$$F = \begin{pmatrix} 0 & 0 & 0 & 0 & S_h\beta_h \\ 0 & 0 & 0 & 0 & 0 \\ 0 & 0 & 0 & 0 & 0 \\ 0 & S_v\beta_v & S_v\beta_v & 0 & 0 \\ 0 & 0 & 0 & 0 & 0 \end{pmatrix} \tag{40}$$

$$V = \begin{pmatrix} A_1 & 0 & 0 & 0 & 0 \\ -\alpha_h & A_2 & 0 & 0 & 0 \\ 0 & -\rho_h & A_3 & 0 & 0 \\ 0 & 0 & 0 & A_5 & 0 \\ 0 & 0 & 0 & -\alpha_V & \mu_V \end{pmatrix} \tag{41}$$

$$FV^{-1} = \begin{pmatrix} 0 & 0 & 0 & \frac{S_h\beta_h\alpha_v}{A_3\mu_v} & \frac{S_h\beta_h}{\mu_v} \\ 0 & 0 & 0 & 0 & 0 \\ 0 & 0 & 0 & 0 & 0 \\ \frac{S_v\beta_v\alpha_h}{A_1A_2} + \frac{S_v\beta_v\alpha_h\rho_h}{A_1A_2A_3} & \frac{S_v\beta_v}{A_2} + \frac{S_v\beta_v\rho_h}{A_2A_3} & \frac{S_v\beta_v}{A_3} & 0 & 0 \\ 0 & 0 & 0 & 0 & 0 \end{pmatrix} \tag{42}$$

$$Det\left|FV^{-1} - \lambda I\right| = R_0 = \sqrt{\frac{A_1A_2A_3A_5\mu_v S_v\beta_v\alpha_h(A_3+\rho_h)S_h\beta_h\alpha_v}{A_1A_2A_3A_5\mu_v}} \tag{43}$$

Substituting the valves of S_h and S_v at HAT-FE, we have

$$R_0 = \sqrt{\frac{\Lambda_v\beta_v\alpha_h(A_3+\rho_h)\Lambda_h\beta_h\alpha_v}{\mu_h\mu_v}} \tag{44}$$

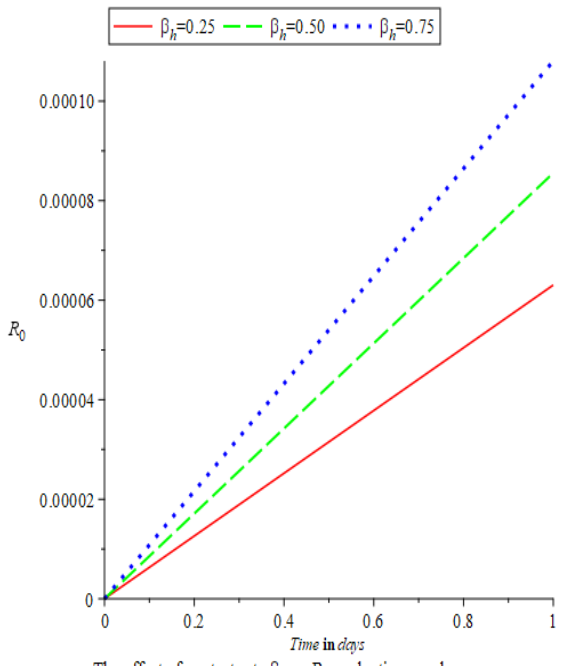

(a) The effect of contact rate β_h on Reproduction number

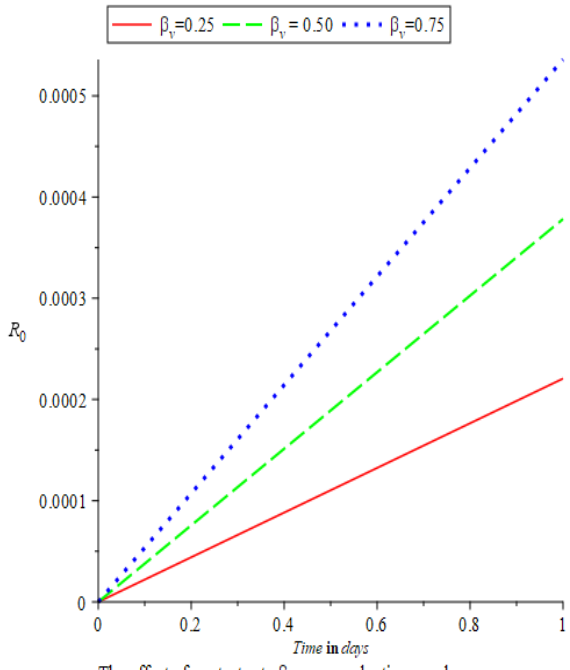

(b) The effect of contact rate β_v on reproduction number

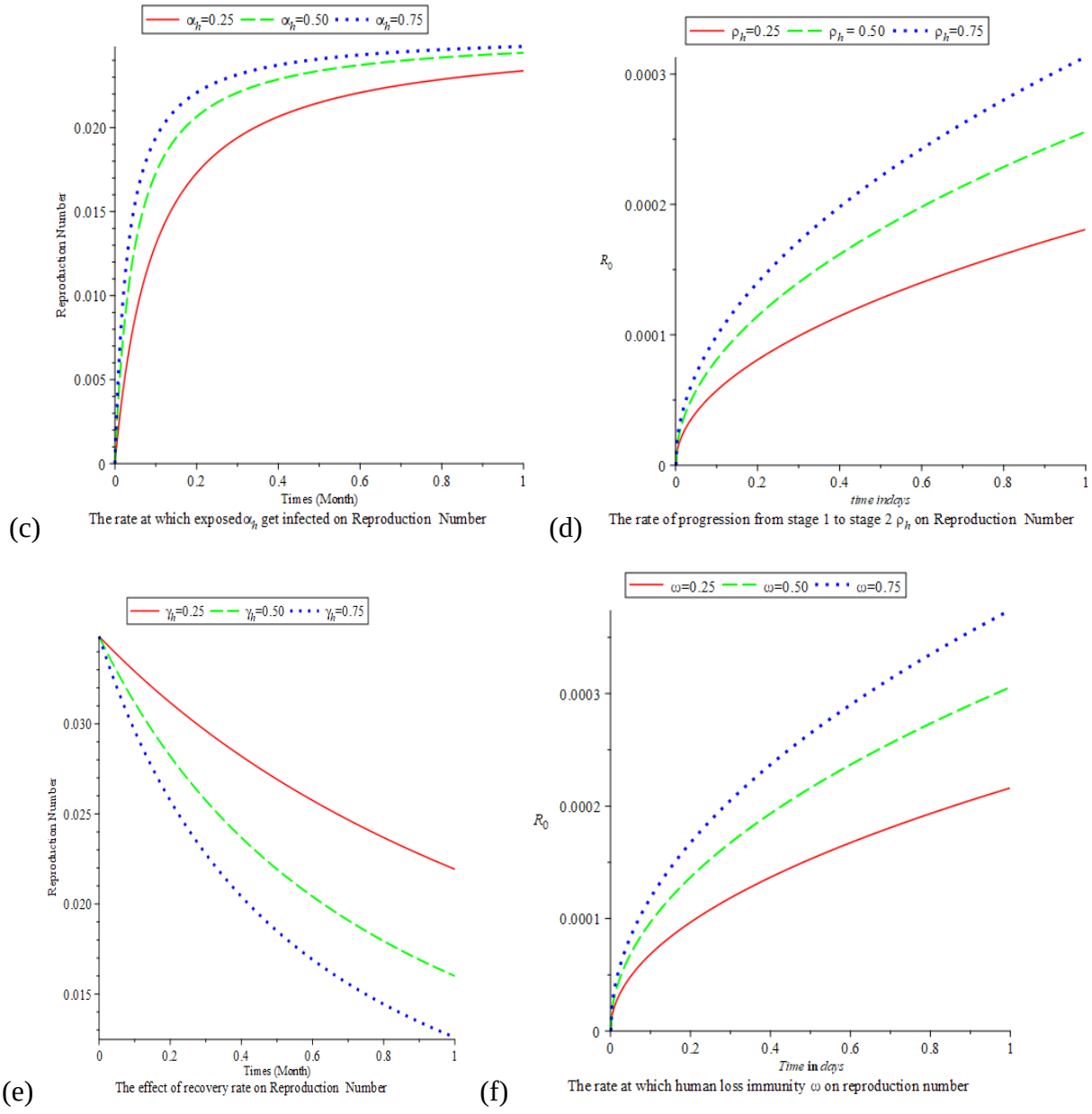

Figure 2: How Some Parameters Affect the Basic Reproduction Number

This figure shows how changes in certain parameters influence the basic reproduction number (R_0).

Graphs (a) and (b) reveal that when the contact rate increases, R_0 also goes up for both humans and tsetse flies. This suggests that more contact between the flies and humans leads to higher exposure to the parasite, increasing the chances of disease spread in both populations.

In graph (c), we see that when the exposure rate rises, the reproduction number also increases. This indicates that the more often humans are exposed to infected vectors, the higher the chance of infection spreading. Graph (d) shows the progression of infection, moving from the early stage to the late stage.

Graph (e) demonstrates that when the recovery rate improves, the reproduction number decreases. This suggests that faster recovery from Human African Trypanosomiasis (HAT) helps reduce its

spread. Conversely, graph (f) shows that if more individuals lose their immunity, the reproduction number rises, making it more likely for the disease to stay circulating within the population.

2.5 Stability Analysis

2.5.1 Local Stability of Disease-Free Equilibrium Point

The disease-free equilibrium (DFE) is generally stable when small disturbances die out over time, which happens when all the eigenvalues of the Jacobian matrix at that point are negative—that is, when the basic reproduction number R_0 is less than 1. However, if any eigenvalue turns out to be positive, then the DFE becomes unstable, meaning the disease can potentially spread.

Proof:
The Jacobian matrix for the system of equations is:

Proof: The Jacobian matrix of the system of equations is:

$$J=\begin{pmatrix} -\mu_h & 0 & 0 & 0 & 0 & 0 & 0 & -S_h\beta_h \\ 0 & -A_1 & 0 & 0 & 0 & 0 & 0 & S_h\beta_h \\ 0 & \alpha_h & -A_2 & 0 & 0 & 0 & 0 & 0 \\ 0 & 0 & \rho_h & -A_3 & 0 & 0 & 0 & 0 \\ 0 & 0 & 0 & \gamma_h & -A_4 & 0 & 0 & 0 \\ 0 & 0 & -S_v\beta_v & 0 & 0 & -\mu_v & 0 & 0 \\ 0 & 0 & S_v\beta_v & 0 & 0 & 0 & -A_5 & 0 \\ 0 & 0 & 0 & 0 & 0 & 0 & 0 & -\mu_v \end{pmatrix} \tag{45}$$

Reducing the matrix (45) to an upper triangular matrix and the characteristic equation gives

$$J=\begin{pmatrix} -\mu_h & 0 & 0 & 0 & 0 & 0 & 0 & -S_h\beta_h \\ 0 & -A_1 & 0 & 0 & 0 & 0 & 0 & S_h\beta_h \\ 0 & 0 & -A_2 & 0 & 0 & 0 & 0 & 0 \\ 0 & 0 & 0 & -A_3 & 0 & 0 & 0 & 0 \\ 0 & 0 & 0 & 0 & -A_4 & 0 & 0 & 0 \\ 0 & 0 & 0 & 0 & 0 & -\mu_v & 0 & 0 \\ 0 & 0 & 0 & 0 & 0 & 0 & -A_5 & 0 \\ 0 & 0 & 0 & 0 & 0 & 0 & 0 & -\mu_v \end{pmatrix} \tag{46}$$

The determinant of equation (46) gives:

$$(-\mu_h-\lambda_1)(-A_1-\lambda_2)(-A_2-\lambda_3)(-A_3-\lambda_4)(-A_4-\lambda_5)(-\mu_V-\lambda_6)(-A_5-\lambda_7)(-\mu_v-\lambda_8)=0 \tag{47}$$

$$\lambda_1=-\mu_h \text{ or } \lambda_2=-A_1 \text{ or } \lambda_3=-A_2 \text{ or } \lambda_4=-A_3 \text{ or } \lambda_5=-A_4 \text{ or } \lambda_6=-\mu_V$$
$$\text{or } \lambda_7=-A_5 \text{ or } \lambda_8=-\mu_v \tag{48}$$

$$\lambda_1=-\mu_h, \lambda_2=-A_1, \lambda_3=-A_2, \lambda_4=-A_3, \lambda_5=-A_4, \lambda_6=-\mu_v, \lambda_7=A_5, \lambda_8=\mu_v \tag{49}$$
$$\lambda_1,\lambda_2,\lambda_3,\lambda_4,\lambda_5,\lambda_6,\lambda_7,\lambda_8<0$$

Since all the eigenvalues of $J(E^0)$ of the DFE are negative, it shows that the system is locally asymptotically stable.

2.5.2 Global Stability

To show that the system tends to settle into a stable state, we use Lyapunov function theory to analyze both the disease-free state and the endemic (disease-present) state.

Global Stability of Disease-Free Equilibrium

Let's start with the disease-free state, labelled as E^0. When the basic reproduction number R_0 is less than or equal to 1, this state is globally stable—that means, no matter where the system begins, it will eventually settle into disease-free conditions.

Theorem 2: The disease-free equilibrium E^0 is globally asymptotically stable (meaning the system will always settle there over time) within the considered region if $R_0 \leq 1$. If R_0 is greater than 1, then this stability does not hold, and the disease can persist or spread.

Proof

Using the Castillo-Chavex theorem [17]. Let $X(t)$ denotes the uninfected population $X = (S_h, R_h, S_v)$, and $Y(t)$ represents the infected, $= (E_h, I_{h1}, I_{h2}, E_v, I_v)$. Thus, system (1) can be written as

$$\frac{dX}{dt} = F(X,Y), \frac{dY}{dt} = G(X,Y); G(X,0) = 0. \tag{50}$$

Where F and G are the corresponding right-hand sides of the system (1). According to [17], to establish the global asymptotic stability of the disease-free equilibrium, the following two conditions (D1) and (D2) must be satisfied for $R_0 < 1$.

- (D1) $X^0 = (1,0,1)^T$ is globally asymptotically stable for $\frac{dX}{dt} = F(X,0)$.
- (D2) $G \geq 0$ where $G(X,Y) = AY - G(X,Y) and\ A = D_Y G(X^0, 0)$ is Metzler matrix $\forall (X,Y) \epsilon \Omega$

The first Condition is the global asymptotic stability of X^0, we have

$$\frac{dX}{dt} = F(X,0) = \begin{pmatrix} \Lambda_h + \omega R_h - \mu_h S_h \\ -(\omega + \mu_h) R_h \\ \Lambda_v - \mu_v S_v \end{pmatrix} \tag{51}$$

By solving the above system, we have the behaviour of each compartment as follows

$$X^0 \begin{pmatrix} S_h \\ R_h \\ S_v \end{pmatrix} = \begin{pmatrix} 1 + S_h(0) e^{-\mu_h t} \\ R_h(0) e^{-(\omega + \mu_h) t} \\ 1 + S_v(0) e^{-\mu_v t} \end{pmatrix} \tag{52}$$

Now since $\lim_{x \to \infty} X(t) = X^0$ satisfying the first condition. For the second condition (D2)

$$A = \begin{pmatrix} -A_1 & 0 & 0 & 0 & 0 \\ \alpha_h & -A_2 & 0 & 0 & 0 \\ 0 & \rho_h & -A_3 & 0 & 0 \\ 0 & S_v \beta_v & S_v \beta_v & -A_5 & 0 \\ 0 & 0 & 0 & \alpha_V & -\mu_V \end{pmatrix} \tag{53}$$

Then we compute

$$G(X,Y) = AY - G(X,Y) = \begin{bmatrix} 0 \\ 0 \\ 0 \\ 0 \\ 0 \end{bmatrix} \tag{54}$$

It is obvious that $G(X,Y) = 0$, thus $G(X,Y) \geq 0$ in (D2) is satisfied. Hence, E^0 is globally asymptotically stable, provided that $R_0 \leq 1$. This completes the proof.

2.5.3 Global Stability of the HAT-present Equilibrium.

The result of the global stability of E^* in this section is as follows.

Theorem 3 The **HAT**-present equilibrium point E^* is globally asymptotically stable (GAS) if $R_0 > 1$.

Proof.

Consider the Lyapunov function

$$L = c_1 S_h + c_2 E_h + c_3 I_{h1} + c_4 I_{h2} + c_5 R_h + c_6 S_v + c_7 E_v + c_8 I_v \tag{55}$$

Where c_i for $i = 1,2,3, \ldots \ldots 8$ are constants to be chosen during the proof are defined. The derivative of L along the solution of (1) is given by

$$\frac{dL}{dt} = c_1 \frac{dS_h}{dt} + c_2 \frac{dE_h}{dt} + c_3 \frac{dI_{h1}}{dt} + c_4 \frac{dI_{h2}}{dt} + c_5 \frac{dR_h}{dt} + c_6 \frac{dS_v}{dt} + c_7 \frac{dE_v}{dt} + c_8 \frac{dI_v}{dt} \tag{56}$$

gives

$$\frac{dL}{dt} = c_1(\Lambda_h + \omega R_h - \beta_h S_h I_v - \mu_h S_h) + c_2(\beta_h S_h I_v - (\alpha_h + \mu_h)E_h) + c_3(\alpha_h E_h - (\rho_h + \mu_h)I_{h1}) + c_4(\rho_h I_{h1} - (\gamma_h + \delta_h + \mu_h)I_{h2}) + c_5(\gamma_h I_{h2} - (\omega + \mu_h)R_h) + c_6(\Lambda_v - \beta_v S_v (I_{h1} + I_{h2}) - \mu_v S_v) + c_7(\beta_v S_v (I_{h1} + I_{h2}) - (\alpha_h + \mu_v)E_v) + c_8(\alpha_v E_v - \mu_v I_v) \tag{57}$$

$$\frac{dL}{dt} = c_1(\Lambda_h - \mu_h S_h) + (c_2 - c_1)\beta_h S_h I_v + (c_3 - c_2)\alpha_h E_h - c_2\mu_h E_h + (c_4 - c_4)\rho_h I_{h1} - c_3\mu_h I_{h1} + (c_5 - c_4)I_{h1} I_{h1} - c_4\gamma_h I_{h2} - c_4\delta_h I_{h2} - \mu_h I_{h2} + (c_5 - c_1)\omega R_h + c_6(\Lambda_v - \mu_v S_v) + (c_7 + c_6)\beta_v S_v (I_{h1} + I_{h2}) - c_5\mu_h R_h + (c_8 - c_7)(\alpha_v E_v - c_7\mu_v E_v - c_8\mu_v I_v \tag{58}$$

Taking $c_1, c_2, c_3, c_4, c_5, c_6, c_7 \; and \; c_8$ such that $c_1 = c_2 = c_3 = c_4 = c_5 = c_6 = c_7 = c_8$, $\Lambda_h - \mu_h S_h = 0$

And $\Lambda_v - \mu_v S_v = 0$ gives

$$\frac{dL}{dt} = c_2\mu_h E_h - c_3\mu_h I_{h1} - c_4\delta_h I_{h2} - c_4\mu_h I_{h2} - c_5\mu_h R_h - c_7\mu_v E_v - c_8\mu_v I_v \tag{59}$$

Since L is positive definite and its time derivative, dL/dt, is negative definite, L acts as a valid Lyapunov function for the system (1). According to Lyapunov's stability theorem [18], the endemic equilibrium E^* is globally asymptotically stable within the invariant region **Ω**.

2.6 Sensitivity Analysis of the Basic Reproduction Number

In this section, we present a brief discussion on the sensitivity analysis of the basic reproduction number R_0. Sensitivity analysis helps identify parameters that significantly influence the threshold ratio R_0. A change in a highly sensitive parameter results in a substantial quantitative shift in R_0 and may even lead to qualitative changes in the system dynamics. These parameters should be prioritized for management strategies and the development of effective control measures.

To quantify sensitivity, we employ the forward sensitivity index, also referred to as the elasticity index Rodrigues, Monteiro, and Torres (2013). This index measures the relative change in R_0 concerning a relative change in a given parameter and is mathematically defined as: R_0^h and R_0^v since they are the basic reproduction numbers for humans and tsetse flies, respectively. The sensitivity analysis of R_0 to each of its parameters will be evaluated via the sensitivities of each R_0^h and R_0^v.

The general sensitivity index is given by:

$$\Upsilon R_0 = \frac{\partial R_0}{\partial p} \times \frac{p}{R_0} \tag{60}$$

Where p is the parameter under consideration

For each component, we compute:

$$\Upsilon R_0^h = \frac{\partial R_0^h}{\partial p_1} \times \frac{p_1}{R_0^h} \quad and \quad \Upsilon R_0^v = \frac{\partial R_0^v}{\partial p_2} \times \frac{p_2}{R_0^v} \tag{61}$$

Table 2: Model Parameters, Baseline Values, and Sources

Parameter	Description	Baseline value	Source
$\boldsymbol{\Lambda_h}$	Recruitment rate of the human population	0.0215	Assumed
$\boldsymbol{\Lambda_v}$	Recruitment rate of the tsetse fly population	0.007	Assumed
$\boldsymbol{\delta_h}$	Disease-induced death	0.0755	Sanda *et al.*, 2024
$\boldsymbol{\mu_h}$	Natural death rate of humans	0.0156	Assumed
$\boldsymbol{\mu_v}$	Natural death rate of the tsetse fly	0.034	Assumed
$\boldsymbol{\beta_h}$	Contact rate of susceptible humans with infected flies	0.62	Ndondo *et al.*, 2016
$\boldsymbol{\beta_v}$	Contact rate of susceptible tsetse fly with an infected human	0.01	Ndondo *et al.*, 2016
$\boldsymbol{\alpha_h}$	The rate at which the exposed human gets infected	0.0013	Assumed
$\boldsymbol{\alpha_v}$	The rate at which the exposed tsetse fly gets infected	0.0252	Sanda *et al.*, 2024
$\boldsymbol{\rho_h}$	Infection progression from stage 1 to stage 2	0.07	Assumed
$\boldsymbol{\gamma_h}$	Rate of recovery from HAT via treatment	0.0125	Assumed
$\boldsymbol{\omega}$	The rate of human loss of immunity and return to susceptibility	0.0140	Sanda *et al.*, 2024

where p_1 and p_2 denote the parameters related to R_0^h and R_0^h, respectively. Using the baseline parameter values in Table 2, the computed sensitivity indices are presented in Table 3.

Parameter	R_0^h Sign	Υe_1	Parameter	R_0^v Sign	Υe_2
β_v	+ve	1.0000	β_h	+ve	1.0000
Λ_h	+ve	0.9999	Λ_v	+ve	0.9999
α_h	+ve	1.0000	α_v	+ve	1.0000
γ_h	+ve	0.1224	μ_v	-ve	0.9999
μ_h	-ve	0.8472			
ρ_h	+ve	0.6856			
δ_h	+ve	0.0392			

The values of the sensitivity indices of R_0^h and R_0^v, corresponding to the human population and the tsetse fly population, respectively, are determined based on their magnitudes and signs, as presented in Table 3. The table shows that the sensitivity indices reveal whether an increase in each parameter leads to an increase or decrease in the basic reproduction number R_0. In general, positive indices suggest that increasing the parameter increases R_0, while negative indices indicate the opposite. These indices reflect the relative significance of each parameter in influencing the spread of the disease in the human and tsetse fly populations. Among all the parameters, the most influential ones on the basic reproduction number are β_h, Λ_h, α_h, β_v, Λ_v, and α_v for both human and tsetse fly. This implies that the population sizes, the contact rates of humans and tsetse flies with the infection, and the progression rates to becoming infected with HAT are the most sensitive factors and are directly proportional to HAT transmission.

3.0 Numerical Simulation

To better understand the behavior of Human African Trypanosomiasis (HAT) transmission between humans and tsetse flies, we used graphical methods to explore how the infection evolves in both populations.

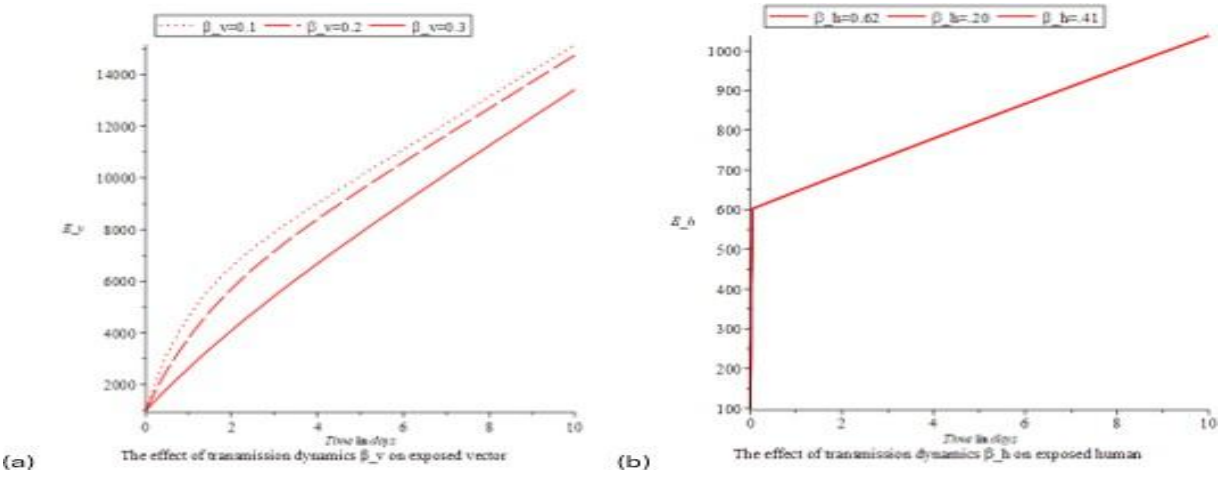

Figure 4. (1a) and 4. (1b) Graphs of the contact rate of human and tsetse fly with infection.

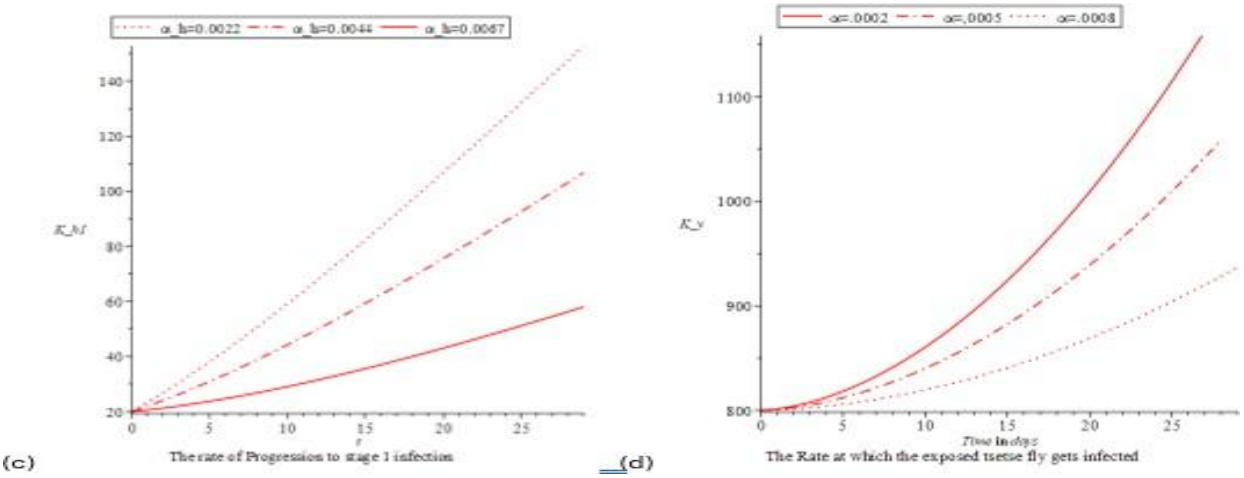

Figure 4. (1c) and 4. (1d) Graphs of transmission dynamics tsetse fly and human

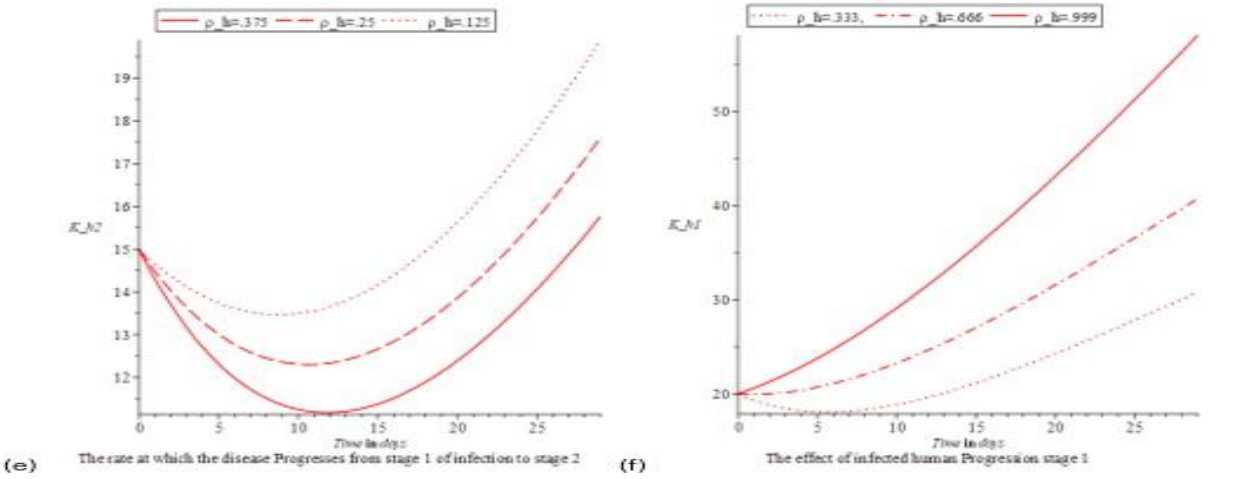

Figure 4.(1e) and 4.(1f) Graphs of diseases progression in human and tsetse fly

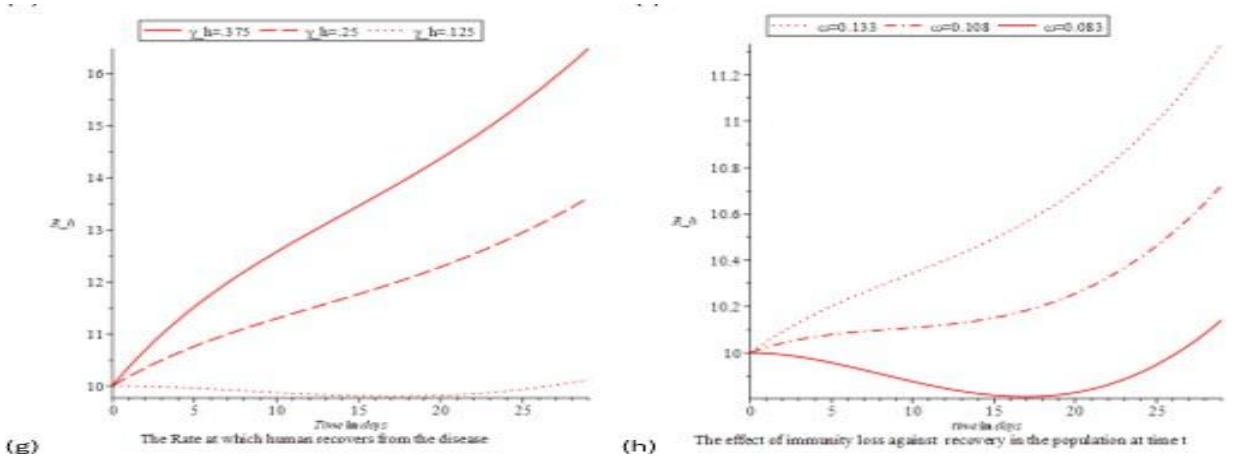

Figure 4. (1g) and 4. (1h) Graphs of human recovery rate and the effect of immunity loss

DISCUSSION OF RESULTS

From Figures 4(a) and (b), we observe a clear pattern as people are increasingly exposed to the parasite, the rate of disease transmission accelerates significantly. For tsetse flies, this means that the more infected flies there are, the more likely it is for humans to become infected. This finding highlights the urgent need for strategies that reduce contact between humans and infected vectors.

Figures 4(c) and 4(d) show that both humans and tsetse flies transition to the infectious stage at similar rates. This suggests a tightly linked cycle of transmission between the two groups, underscoring the importance of breaking this cycle through early intervention in both human and vector populations.

Figures 4(e) and 4(f) show how the disease progresses through different stages. In Figure 4(f), we see that during the early (acute) stage, symptoms may be mild, and diagnosis can be delayed, yet the disease remains transmissible. Figure 4(e), on the other hand, represents the later (critical) stage of the disease, where symptoms are severe and, without timely and appropriate treatment, can lead to fatal outcomes. This reinforces the need for increased awareness, early detection, and rapid response systems in endemic areas.

Figure 4(g) provides hope: With proper treatment, recovery from Human African trypanosomiasis (HAT) can be fast and effective. However, Figure 4(h) shows a concerning trend of recovered individuals quickly losing immunity and becoming susceptible to infection again. This highlights a key policy gap: the urgent need to invest in vaccine research and development to provide long-term or permanent immunity, which could dramatically reduce the burden of HAT.

CONCLUSION

Mathematical Modeling of Human African Trypanosomiasis (HAT) Transmission Dynamics with Two Stages of Infection was considered. The findings highlight the dynamics of transmission between humans and tsetse flies. We investigate the solutions of the model to make sure they make biological and mathematical sense, specifically, that they stay positive and within reasonable limits. We calculated both the disease-free and disease endemic equilibrium points and analyzed their stability. Additionally, we derived the basic reproduction number, R_0, which acts as a key threshold: if R_0 is less than 1, the disease is likely to die out; if it's greater than 1, the disease may persist. Our sensitivity analysis also identified which parameters have the biggest influence on the system's stability, highlighting the importance of the transmission rate of HAT and the rate at which people relapse. Numerical simulations were carried out, and the graphs were plotted and discussed. However, the need for some control measures to be put in place, such as timely diagnosis, prompt treatment, and effective vector control, is essential to reducing the HAT burden. The rapid loss of immunity after recovery points to a critical need for long-term solutions, particularly vaccine development. These insights call for a coordinated policy response that includes public health education, vector control, improved healthcare access, and investment in vaccine development to reduce the long-term impact of Human African Trypanosomiasis (HAT) on affected communities.

REFERENCES

[1] A. M. Ndondo, J. M. W. Munganga, J. N. Mwambakana, C. M. Saad-Roy, P. van den Driessche, and R. O. Walo, “Analysis of a model of Gambiense sleeping sickness in humans and cattle,” *J. Biol. Dyn.*, vol. 10, no. 1, pp. 347–365, 2016, doi: 10.1080/17513758.2016.1190873.

[2] J. Rodgers, I. Steiner, and P. G. E. Kennedy, “Generation of neuroinflammation in human African trypanosomiasis,” vol. 0, 2019, doi: 10.1212/NXI.0000000000000610.

[3] C. Brun, R., Blum, J., Chappuis, F., & Burri, “Human african try- panosomiasis,” *Lancet*, vol. 375, no. (9709), p. 375 (9709), 2010.

[4] A. G. Kermack, W. O., & McKendrick, “A contribution to the mathematical theory of

epidemics," *R. Soc. London. Ser. A*, vol. 115, no. 772, pp. 700–721, 1927.

[5] J. A. J. Diekmann, O., Heesterbeek, J. A. P., & Metz, "On the definition and the computation of the basic reproduction ratio r 0 in models for infectious diseases in heterogeneous populations," *J. Math. Biol.*, vol. 28, pp. 365–382, 1990.

[6] M. E. Newman, "Spread of epidemic disease on networks," *Phys. Rev.. E*, vol. 66, no. 1, p. 016128, 2002.

[7] L. Halloran, M. E., Longini, I. M., Struchiner, C. J., Halloran, M. E. and C. J. I. M., & Struchiner, "Overview of vaccine effects and study designs," *Des. Anal. Vaccine Stud.*, pp. 19–45, 2010.

[8] D. S. Ferguson, N. M., Cummings, D. A., Fraser, C., Cajka, J. C., Cooley, P. C., & Burke, "Strategies for mitigating an influenza pandemic," *Nature*, vol. 442, no. 7101, pp. 448–452, 2006.

[9] H. A. Abioye, A. I., Ibrahim, M. O., Peter, O. J., & Ogunseye, "Optimal control on a mathematical model of malaria," *Sci. Bull., Ser. A Appl Math Phy*, vol. 82, no. 3, pp. 177–190, 2020.

[10] F. Weidemann, "Optimal control on a mathematical model of malaria," 2015.

[11] J. W. Hargrove, R. Ouifki, D. Kajunguri, G. A. Vale, and S. J. Torr, "Modeling the control of trypanosomiasis using trypanocides or insecticide-treated livestock," *PLoS Negl. Trop. Dis.*, vol. 6, no. 5, 2012, doi: 10.1371/journal.pntd.0001615.

[12] G. Liana, Y. A., Shaban, N., & Mlay, "Modeling optimal control of african trypanosomiasis disease with cost-effective strategies," *J. Biol. Syst.*, vol. 29, no. 04, pp. 823–848, 2021.

[13] H. E. Gervas, N. K. D. O. Opoku, and S. Ibrahim, "Mathematical Modelling of Human African Trypanosomiasis Using Control Measures," *Comput. Math. Methods Med..*, vol. 2018, 2018, doi: 10.1155/2018/5293568.

[14] M. O. Onuorah, A. B. Namwanje, Neoline, and A. M. Baba "Optimal Control Model of Human African Trypanosomiasis," *World Sci. News*, vol. 178, no. February, pp. 136–153, 2023.

[15] M. Helikumi and S. Mushayabasa, "Mathematical modeling of trypanosomiasis control strategies in communities where human, cattle and wildlife interact," *Anim. Dis.*, vol. 3, no. 1, pp. 1–15, 2023, doi: 10.1186/s44149-023-00088-6.

[16] P. Van Den Driessche and J. Watmough, "Reproduction numbers and sub-threshold endemic equilibria for compartmental models of disease transmission," *Math. Biosci.*, vol. 180, no. 1–2, pp. 29–48, 2002, doi: 10.1016/S0025-5564(02)00108-6.

[17] et al. Castillo-Chavez, C., Feng, Z., Huang, W., "On the computation of r (o) and its role on global stability." 2001.

[18] P. Rakkiyappan, R., & Balasubramaniam, "Delay-dependent asymptotic stability for stochastic delayed recurrent neural networks with time varying delays," *Appl. Math. Comput.*, vol. 198, no. 2, pp. 526–533, 2008.